Supplemental Information

iPSC-Derived Human Microglia-Like Cells to Study Neurological Diseases

Edsel M. Abud, Ricardo N. Ramirez, Eric S. Martinez, Luke M. Healy, Cecilia H.H. Nguyen, Sean A. Newman, Andriy V. Yeromin, Vanessa M. Scarfone, Samuel E. Marsh, Cristhian Fimbres, Chad A. Caraway, Gianna M. Fote, Abdullah M. Madany, Anshu Agrawal, Rakez Kayed, Karen H. Gylys, Michael D. Cahalan, Brian J. Cummings, Jack P. Antel, Ali Mortazavi, Monica J. Carson, Wayne W. Poon, and Mathew Blurton-Jones

Supplemental Figures

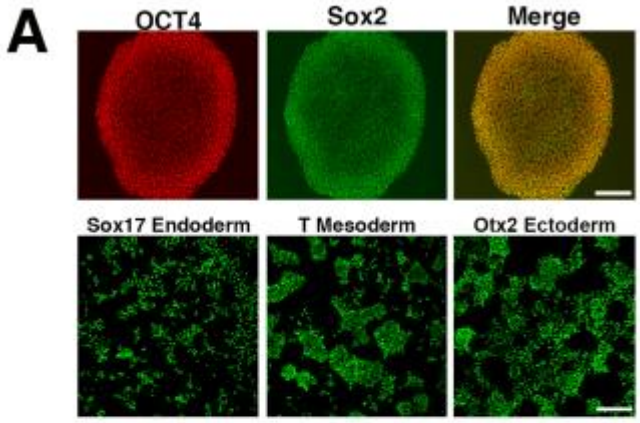

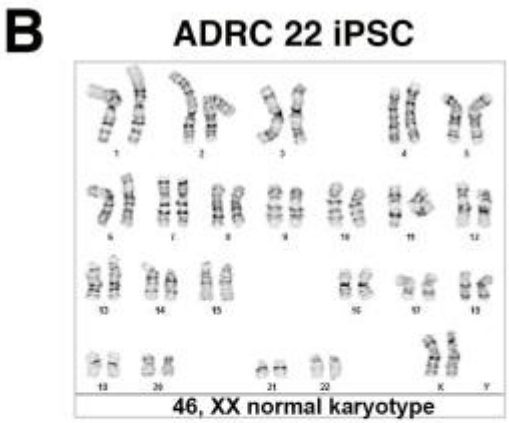

C

iPSC ID	Source	iPSC Karyotype	Sex	Pluritest Score	Pluritest (pass vs. fail)	Novelty Score	Novelty (pass vs. fail)
ADRC iPS 2	Fibroblast	46 XY normal	Male	19.29	Pass	1.511	Pass
ADRC iPS 4	Fibroblast	46 XY normal	Male	23.09	Pass	1.449	Pass
ADRC iPS 5	Fibroblast	46 XX normal	Female	21.85	Pass	1.409	Pass
ADRC iPS 12	PBMC	46 XY normal	Male	26.45	Pass	1.519	Pass
ADRC iPS 14	Fibroblast	46 XY normal	Male	26.85	Pass	1.418	Pass
ADRC iPS 20	Fibroblast	46 XX normal	Female	27.19	Pass	1.376	Pass
ADRC iPS 22	Fibroblast	46 XX normal	Female	22.82	Pass	1.404	Pass
ADRC iPS 76	PBMC	46 XY normal	Male	21.37	Pass	1.433	Pass
ADRC iPS 85	Fibroblast	46 XY normal	Male	33.73	Pass	1.325	Pass
ADRC iPS 86	Fibroblast	46 XX normal	Female	32.70	Pass	1.276	Pass

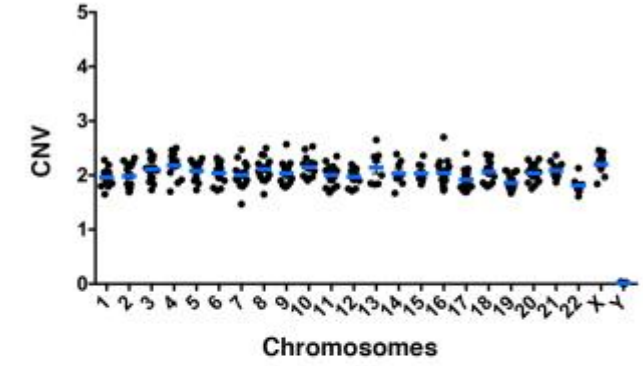

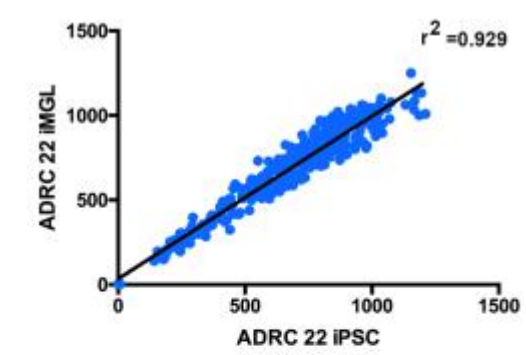

E

ID	Karyotype	Sex	Aneuploidy
iPSC			
ADRC iPS 5	46 XX normal	Female	No
ADRC iPS 14	46 XY normal	Male	No
ADRC iPS 22	46 XX normal	Female	No
ADRC iPS 76	46 XY normal	Male	No
ADRC iPS 76 Replicate	46 XY normal	Male	No
CDI iHPC	46 XY normal	Male	No
iMGL			
ADRC iMGL 5	46 XX normal	Female	No
ADRC iMGL 14	46 XY normal	Male	No
ADRC iMGL 22	46 XX normal	Female	No
ADRC iMGL 76	46 XY normal	Male	No
ADRC iMGL 76 Replicate	46 XY normal	Male	No
CDI iMGL	46 XY normal	Male	No

Figure S1. **Related to Figure 1. Genomic stability of iPSCs and iMGLs.** (**A**) Top: Representative fluorescent images of iPSCs expressing the pluripotent markers OCT4 (red) and SOX2 (green). Scale bar =300 μm. Bottom: Functional validation of pluripotency in iPSCs. Representative fluorescent images of iPSCs differentiated to endoderm, mesoderm and ectoderm and stained for Sox17, T (Brachyury), and Otx2 respectively to validate differentiation potential. Scale bar =200 μm. (**B-C**) Karyotype and Pluritest scores indicate all iPSC lines generated using Sendai virus and used in this study were karyotypically normal and pluripotent. The Pluritest is a microarray-based assessment of pluripotency based on iPS whole transcriptome analysis referenced to a library of functionally validated iPSCs (Muller, F.J. et al. 2011). (**D-E**) Maintenance of genomic stability over the course of iMGL differentiation using pluripotent iPS or commercial hematopoietic progenitors. CNV assessment of differentiated iMGLs reveals genomic stability is maintained over the course of differentiation. (**D**) Representative Nanostring nCounterKaryotype results demonstrate that microglia derived from ADRC iPS line 22 do not inherit extrachromosomal DNA over the course of differentiation. (**E**) Quantification of the 338 probe sets across all 24 chromosomes do not reveal any chromosomal abnormalities (n=6). (**F**) Representative analysis of iMGL derived from its iPSC show strong CNV correlation (r^2=0.929) showing sensitivity of assay and genomic stability of derived iMGLs.

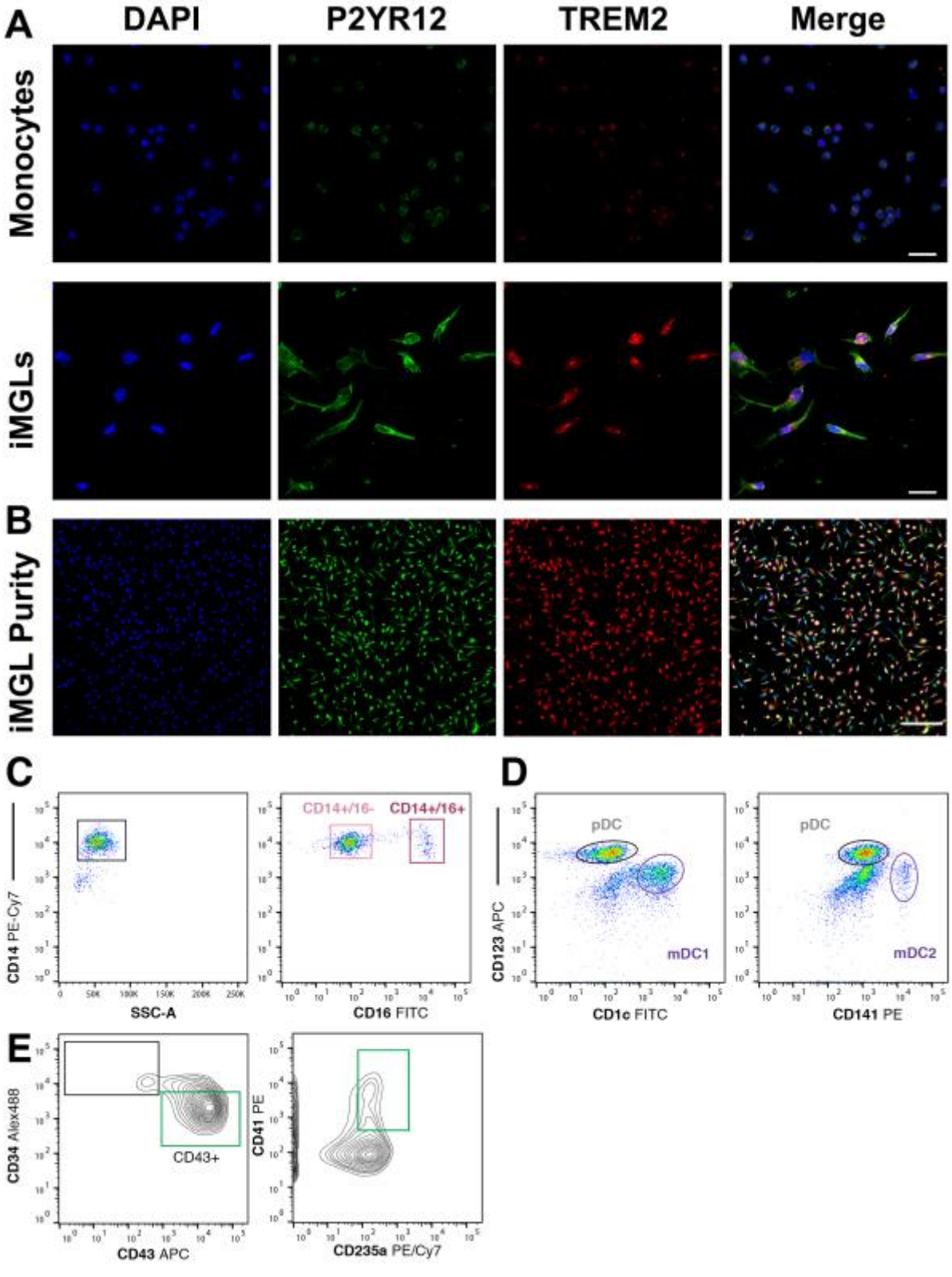
A
DAPI
P2YR12
TREM2
Merge
Monocytes
iMGLs
B
iMGL Purity
C
CD14 PE-Cy7
SSC-A
CD14+/16-
CD14+/16+
CD16 FITC
D
pDC
mDC1
mDC2
CD123 APC
CD1c FITC
CD141 PE
E
CD34 Alex488
CD43+
CD43 APC
CD41 PE
CD235a PE/Cy7

Figure S2. Related to Figures 1 and 2. Assessment of iMGL purity by P2RY12/TREM2 co-localization and flow cytometry characterization of monocytes, dendritic cells and commercial iHPCs. (**A**) Specificity assessment of rabbit anti-human P2ry12 (HPA014518, also recently validated by (Mildner et al., 2017), and goat anti-human Trem2 (R&D, AF1828) in human monocytes and iMGLs. scale bar = 20 μm (**B**) Representative immunofluorescent images (from 5 representative lines) of iMGL purity by P2ry12/Trem2/DAPI co-localization. scale bar = 100μm (**C**) Human $CD14^{+}/CD16^{-}$ monocytes and $CD14^{+}/CD16^{+}$ inflammatory monocytes, CD14M and CD16M respectively, were isolated from young healthy human blood (18-39 y.o.) by FACS. Cells were first gated on viability (not shown), then CD14 to avoid contaminating leukocytes, and finally sorted according to CD16 expression and collected for RNA. (**D**) Human myeloid dendritic cells (Blood DCs) were isolated from young healthy human blood (18-39 y.o.) using untouched myeloid DC enrichment kit followed by FACS. To avoid plasmacytoid DC contamination, DCs were stained for CD123, and myeloid DC subtypes CD1c, and C141 were collected for RNA. (**E**) A commercial iPSC-HPC source ($CD43^{+}/235a^{+}/CD41^{+}$) cells were identified and used to compare to in-house iHPC differentiation and further iMGL differentiation.

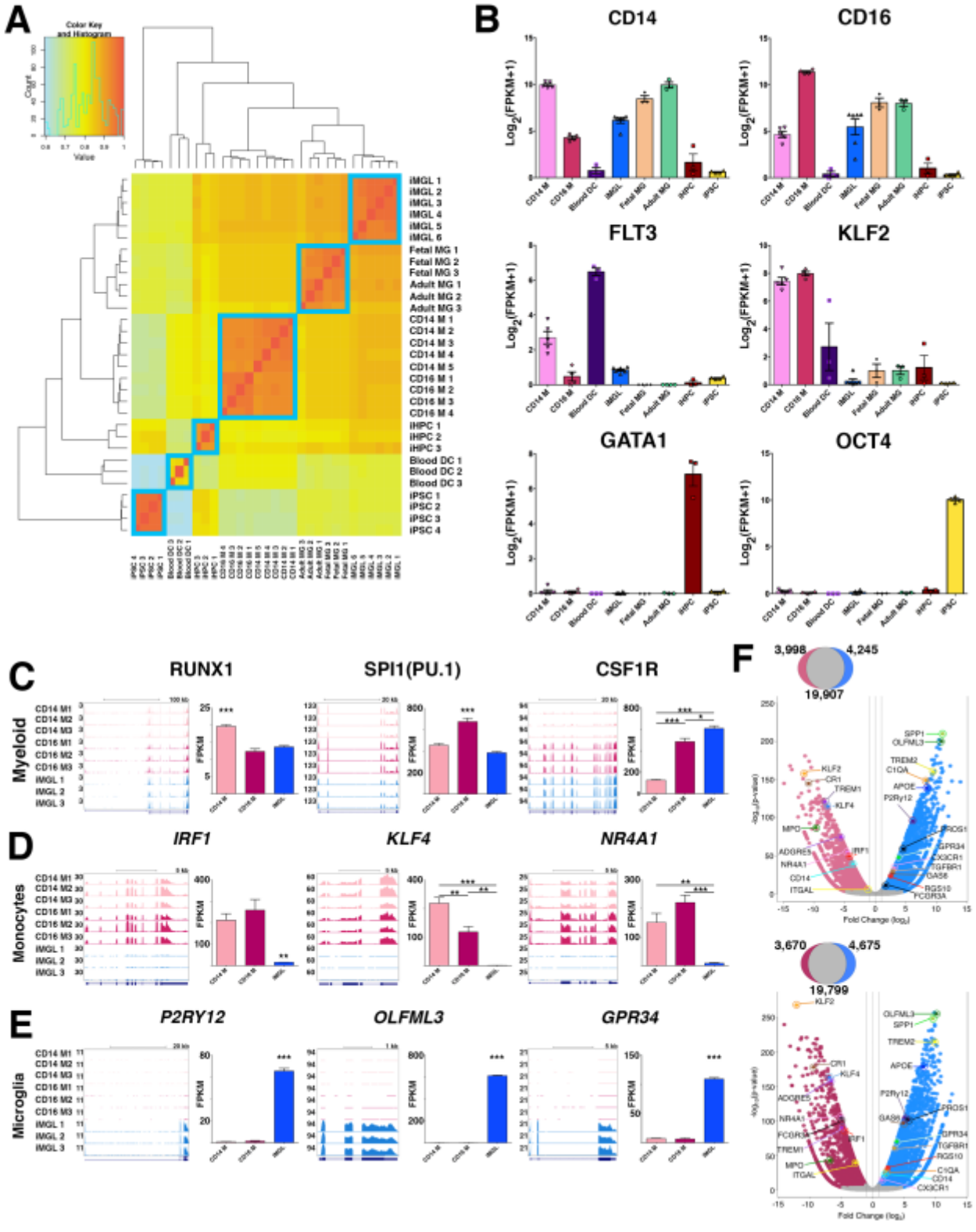
A
Color Key and Histogram
Count
Value
iMGL 1
iMGL 2
iMGL 3
iMGL 4
iMGL 5
iMGL 6
Fetal MG 1
Fetal MG 2
Fetal MG 3
Adult MG 1
Adult MG 2
Adult MG 3
CD14 M 1
CD14 M 2
CD14 M 3
CD14 M 4
CD14 M 5
CD16 M 1
CD16 M 2
CD16 M 3
CD16 M 4
iHPC 1
iHPC 2
iHPC 3
Blood DC 1
Blood DC 2
Blood DC 3
iPSC 1
iPSC 2
iPSC 3
iPSC 4
B
CD14
CD16
FLT3
KLF2
GATA1
OCT4
Log2(FPKM+1)
C
RUNX1
SPI1(PU.1)
CSF1R
Myeloid
FPKM
D
IRF1
KLF4
NR4A1
Monocytes
E
P2RY12
OLFML3
GPR34
Microglia
F
3,998
4,245
19,907
3,670
4,675
19,799
Fold Change (log2)

Figure S3. Related to Figure 2. Correlational Matrix of biological samples used in RNA-sequencing and iMGL gene example genes. (**A**) Spearmen correlational matrix of biological samples used in RNA-sequencing highlights strong intra-group correlation. iMGLs correlate well with Fetal and Adult MGs suggesting strong gene expression similarity between samples. (**B**) Histograms of key genes found across different samples. CD14 and FCGR3A (also known as CD16) expressed in all myeloid cells including microglia, although enriched in CD14 M and CD16 M, respectively. As expected, FLT3 is highly expressed in Blood DCs and not in other cells and is barely detected in all three microglia groups. The monocyte/macrophage-specific transcription factor KLF2 was enriched in only CD14 M and CD16 M. Whereas GATA1 and OCT4 were only detected in iHPCs and iPSCs, respectively. (**C**-**F**) RNA-sequencing expression profile of iMGL reveals they are unique from $CD14M^-$ and CD16M and highly express microglial genes. (**C**-**E**) RNA-seq coverage maps and gene FPKM values in CD14 M, CD16 M, and iMGL for (**C**) for the myeloid genes RUNX1, PU.1, and CSF1R (**D**) monocyte-enriched genes IRF1, KLF4, and NR4A1 and (**E**) microglial-enriched genes P2RY12, OLFML3, and GPR34 in iMGL. For all RNA coverage maps, the y-axis represents Reads Per Million (RPM) scaled accordingly for all samples. Histogram comparisons using FPKM values for all genes are shown as the mean± s.e.m. Biological replicates for CD14 M (n=5), CD16 (n=4), and iMGL (n=6) are included for comparison by one-way ANOVA followed by Turkey's multiple-comparison post-hoc test. (**F**) Representative volcano plots of differentially expressed genes (p-value < 0.001, two-fold change) in iMGL (blue), CD14 M (light pink), and non-significant (grey). Key genes are both colored and labeled uniquely. Fold change (log_2) and $-log_{10}$(p-value) indicate the x and y-axis respectively. Grey dashed vertical lines indicate a two-fold change in gene expression. Venn diagrams indicate total number of differentially expressed genes for each condition. **p<0.001, ***p<0.0001.

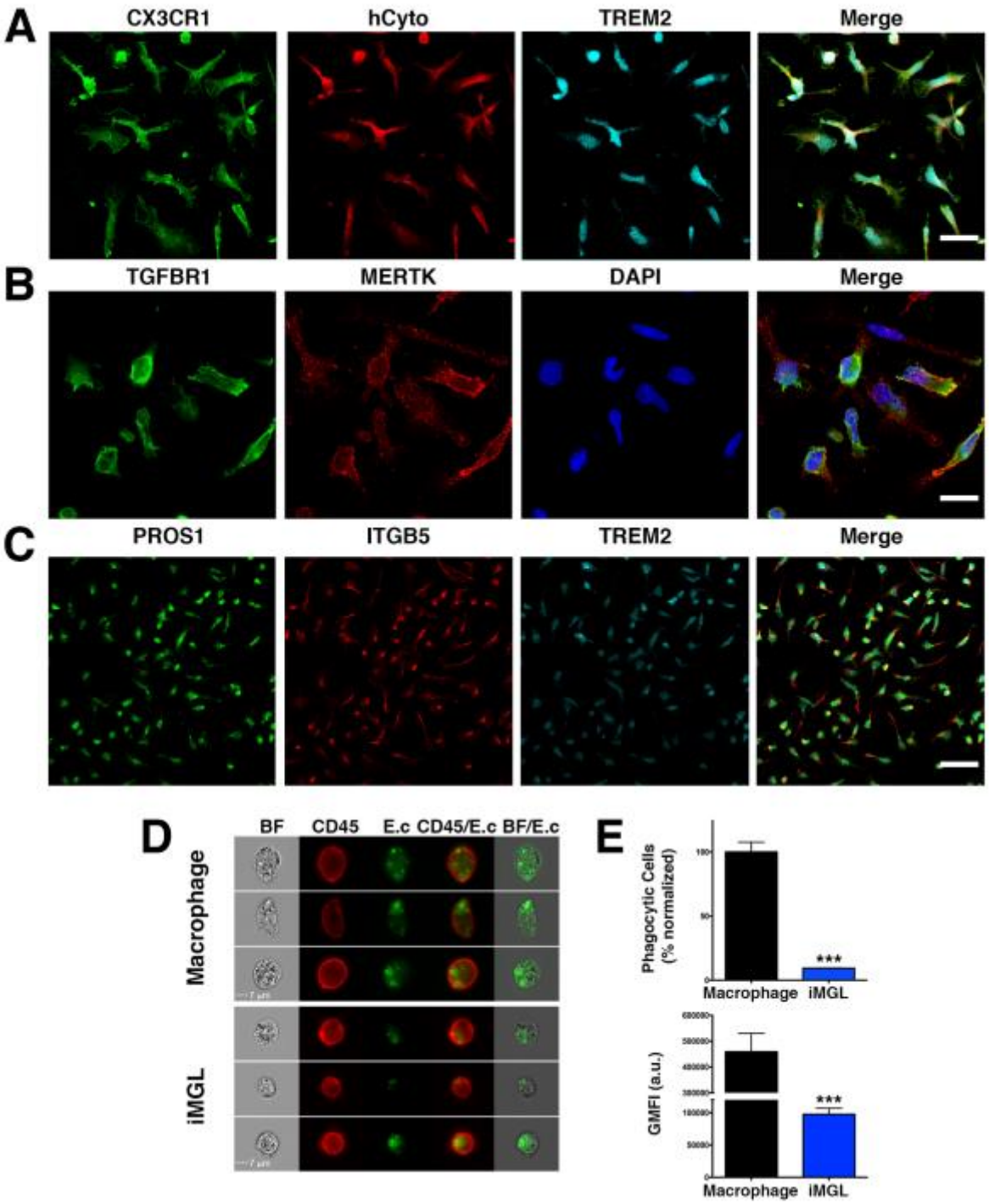

Figure S4. Related to Figure 3. iMGLS are positive for microglia surface proteins and perform phagocytosis of *E. coli* particles. Representative immunofluorescent images of iMGL expressing microglial markers (**A**) CX3CR1 (green), hCyto (human cytoplasm marker, SC121; red), TREM2 (cyan). scale bar = 20 μm (**B**) Co-localization of TGFBR1(green), MERTK (red), nuclei (DAPI, blue) scale bar = 20 μm. (**C**) PROS1 (green), ITGB5 (red), TREM2 (cyan). scale bar = 100 μm (**D-E**) Assessment of phagocytosis of pHrodo-labeled *E. coli* (E.c; green) (**D-E**) in human monocyte-derived macrophages (black) and iMGLs (blue). (**D**) Representative bright field

and immunofluorescent images captured by Amnis Imagestream flow cytometer visualizing phagocytosis of E.c within macrophages (top) and iMGL (bottom). (**E**) Quantification of percent phagocytic cells (top) reveals that iMGLs (blue) phagocytose E.c almost 10-fold less frequently than macrophages (black) as expected. (**B:** bottom) The amount of E.c internalized (by GMFI) within phagocytic cells further illustrates the greater phagocytic capacity of macrophages compared to iMGLs. , n=3/group. Student's T-test,*** $p<0.001$.

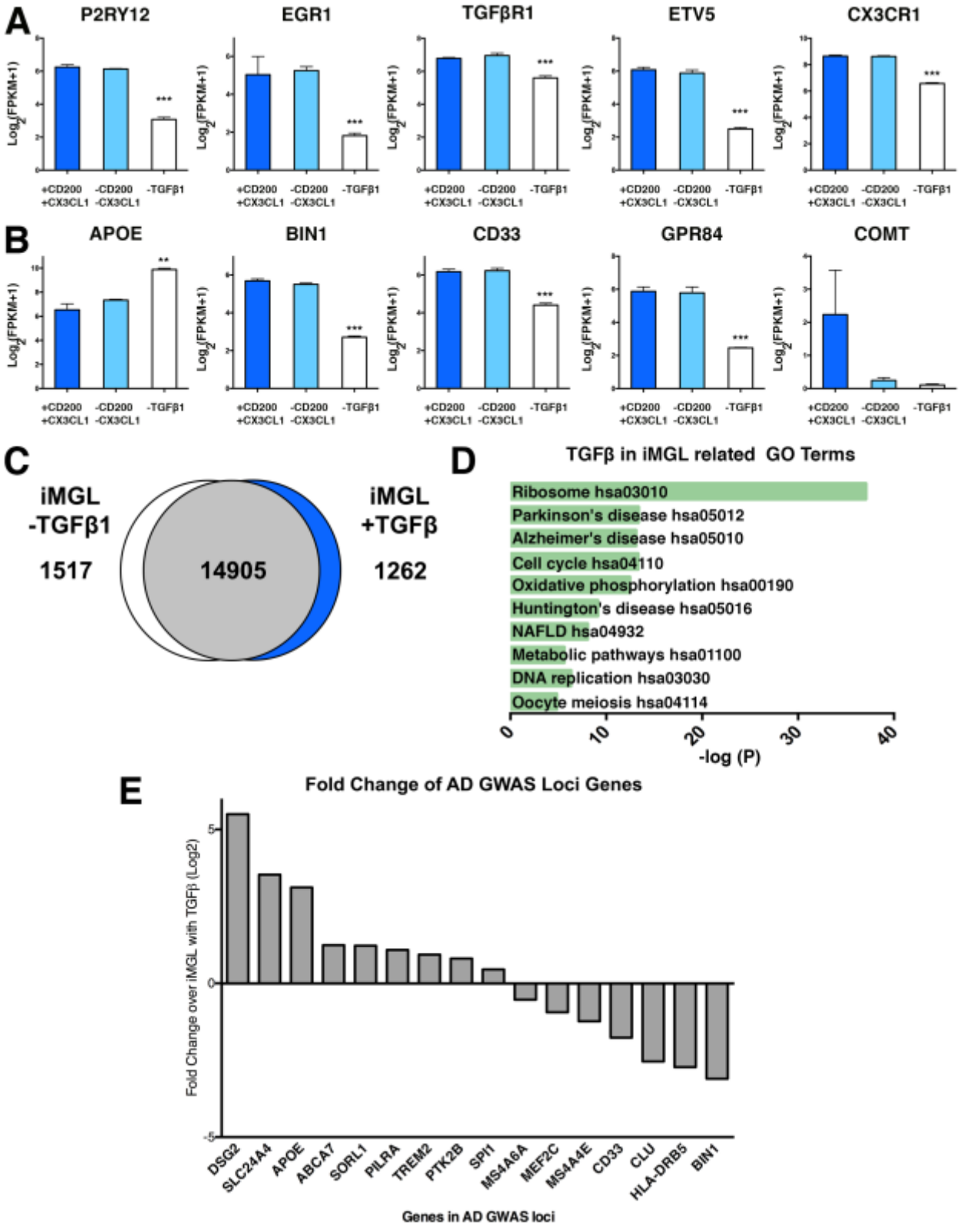
A
P2RY12
EGR1
TGFβR1
ETV5
CX3CR1
B
APOE
BIN1
CD33
GPR84
COMT
Log2(FPKM+1)
+CD200 +CX3CL1
-CD200 -CX3CL1
-TGFβ1
C
iMGL -TGFβ1
1517
14905
iMGL +TGFβ
1262
D
TGFβ in iMGL related GO Terms
Ribosome hsa03010
Parkinson's disease hsa05012
Alzheimer's disease hsa05010
Cell cycle hsa04110
Oxidative phosphorylation hsa00190
Huntington's disease hsa05016
NAFLD hsa04932
Metabolic pathways hsa01100
DNA replication hsa03030
Oocyte meiosis hsa04114
-log (P)
E
Fold Change of AD GWAS Loci Genes
Fold Change over iMGL with TGFβ (Log2)
DSG2
SLC24A4
APOE
ABCA7
SORL1
PILRA
TREM2
PTK2B
SPI1
MS4A6A
MEF2C
MS4A4E
CD33
CLU
HLA-DRB5
BIN1
Genes in AD GWAS loci

Figure S5. Related to Figures 2 and 4. TGFβ-1, CX3CL1, CD200 and their impact on key microglial genes are associated with modulating neuronal function and environment. (**A**-**B**) TGFβ1 maintains core microglial genes. Withdrawal of TGFβ1 for 24 h (white bars) strongly influences microglial transcriptome. In agreement with mouse studies *in vivo* (Butovsky, et al, 2014), TGFβ removal reduces expression of key microglia genes including surface receptors P2RY12, TGFβR1, and CX3CR1, while also reducing expression of microglia transcription factors EGR1 and ETV5. AD-associated pathway genes such as BIN1, CD33, and APOE are also influenced by the lack of TGFβ. Removal of CX3CL1 and CD200, does not change core microglia identity, but impacts state by influencing homeostatic gene expression such as, COMT, and APOE (*B*). (**C**) Differential gene expression analysis reveals that presence of TGFβ increases expression of 1262 genes in iMGLs, while lack of TGFβ reduces expression of 1517 genes, further supporting previous work highlighting the role of TGFB in microglia development, gene signature, and function. (**D**) KEGG pathway analysis highlights that microglial-core genes, elevated with TGFβ, modulate pathways in CNS disease including Alzheimer's, Parkinson's, and Huntington's disease. Statistics reflect one-way ANOVA followed by Dunnett's multiple-comparison post-*hoc* test. * $p<0.05$, ** $p<0.001$, *** $p<0.0001$.

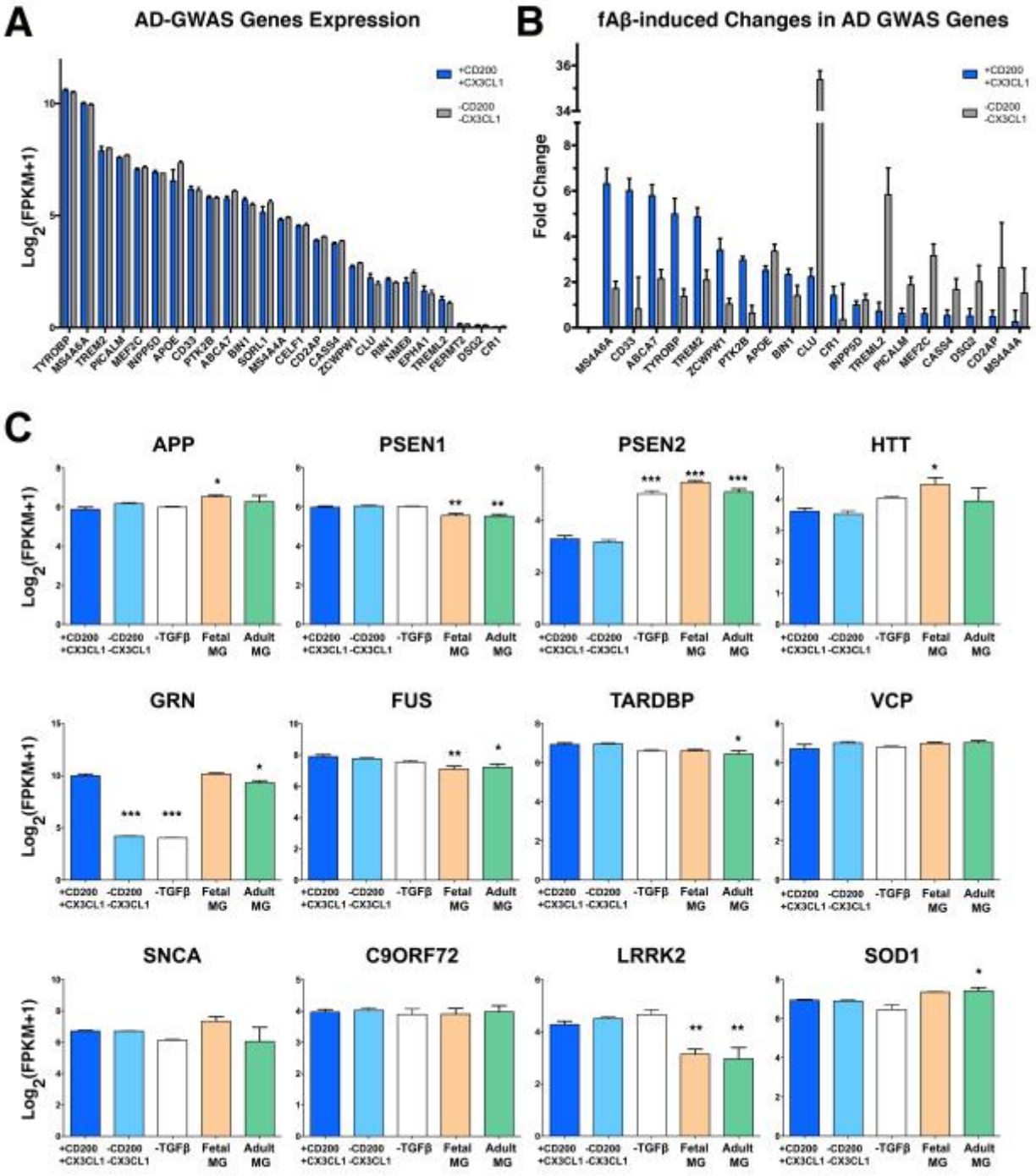

Figure S6. Related to Figures 4 and 5. Microglia AD-GWAS and other CNS-disease related genes can be studied using iMGLs. (**A-B**) iMGL AD-related GWAS genes respond to fAβ differentially if primed with or without CD200 and CX3CL1. iMGL exposure to CNS factors, CD200 and CX3CL1, "primes" their response to fAβ by increasing expression of genes with functions implicated to modulate microglia inflammation and function in AD, like CD33, ABCA7, TYROBP, and TREM2. Stimulation with fAβ of iMGLs not exposed to CD200 or CX3CL1 results in increase expression of AD GWAS-related genes CLU and APOE, genes involved in response

to misfolded proteins as well as survival and homeostasis. (**C**) Major neurodegenerative related genes, APP (AD), SCNA (PD) and HTT (HD), are expressed in iMGLs and primary microglia. iMGLs also express genes linked to Amylotrophic Lateral Sclerosis (ALS), Frontal-temporal Dementia (FTD), and Dementia with Lewy Bodies (DLB) and support previous studies implicating microglia dysfunction**.** Bar graphs of genes implicated in neurodegenerative diseases that are detected in iMGL similarly to Fetal and Adult MG, and expressed as Log_2 (FPKM +1) and presented as mean ± SEM. Like isolated human primary microglia, iMGLs express Valosin Containing Protein (VCP), FUS binding protein (FUS), proganulin (GRN), TDP-43 (TARDBP), LRRK2, and Superoxide Dismutase (SOD). Recent literature implicates microglia dysfunction related to mutations or loss of function of these genes playing a role in the pathogenesis of ALS (SOD1, TARDBP, FUS), FTD (VCP, GRN, TARDBP), PD (LRRK2, SNCA), and DLB (SNCA), suggesting the utility of iMGLs in studying the underlying mechanism of these genes in these neurological diseases. Statistics reflect one-way ANOVA followed by Turkey's multiple-comparison *post-hoc* test. * $p<0.05$, ** $p<0.001$, *** $p<0.0001$.

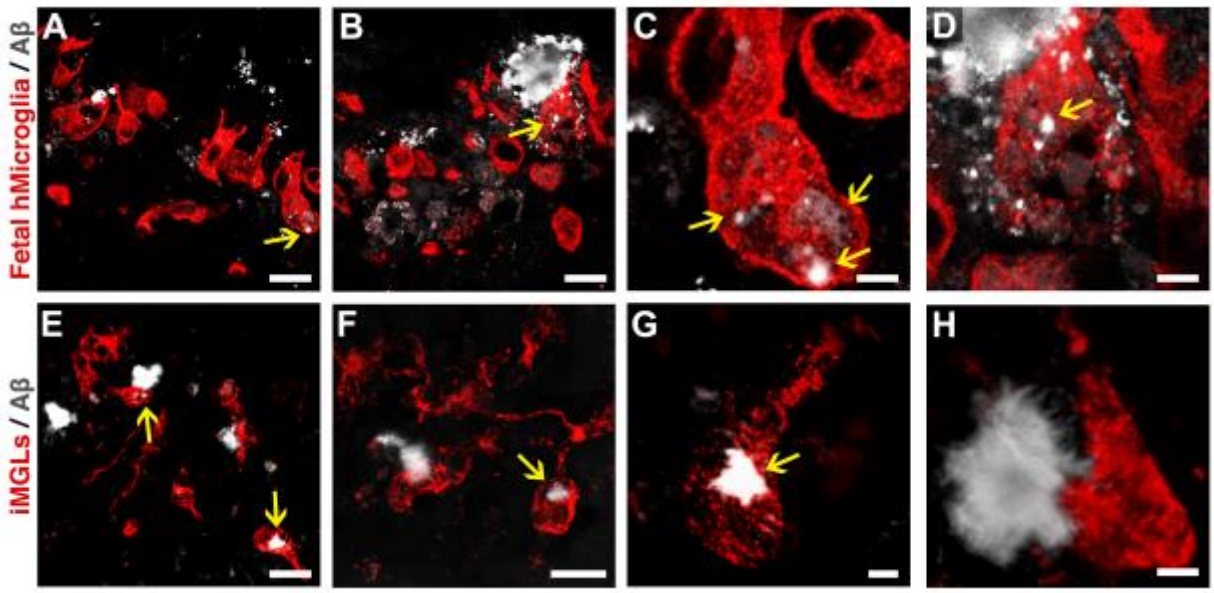

Figure S7. Related to Figure 7. iPS-derived microglial cells engraft and phagocytose Aβ like human fetal microglia. (**A-D**) Human fetal microglia (hCyto, red) were transplanted into immune deficient AD mouse model, Rag5xfAD, (Marsh et al., 2016), and respond to beta-amyloid plaques. Fetal microglia are observed surrounding plaques (**C**), and phagocytosing Aβ (yellow arrows; **C-D**). (**E-H**) Like fetal microglia, iMGLs (hCyto, red) surround and phagocytose (yellow arrows) beta-amyloid plaques. Scale bars (A, B, E, F) = 20 μm, (C, D, H, G) 5 μm.

Table S1: Adjusted *p*-values for 12 genes across all groups.

	GENES					
COMPARISONS	**P2RY12**	**GPR34**	**CABLES1**	**BHLHE41**	**TREM2**	**OLFML3**
CD14+ M VS. CD16+ M	0.7965	> 0.9999	> 0.9999	> 0.9999	0.9987	0.9871
CD14+ M VS. BLOOD DC	0.7531	0.0063	0.5606	> 0.9999	0.6405	> 0.9999
CD14+ M VS. IMGL	< 0.0001	< 0.0001	< 0.0001	0.0064	< 0.0001	< 0.0001
CD14+ M VS. FETAL MG	< 0.0001	< 0.0001	< 0.0001	< 0.0001	< 0.0001	< 0.0001
CD14+ M VS. ADULT MG	< 0.0001	< 0.0001	< 0.0001	< 0.0001	< 0.0001	< 0.0001
CD16+ M VS. BLOOD DC	0.2047	0.0129	0.6603	> 0.9999	0.8586	0.9976
CD16+ M VS. IMGL	< 0.0001	< 0.0001	< 0.0001	0.0111	< 0.0001	< 0.0001
CD16+ M VS. FETAL MG	0.0004	< 0.0001	< 0.0001	< 0.0001	< 0.0001	< 0.0001
CD16+ M VS. ADULT MG	0.0002	< 0.0001	< 0.0001	< 0.0001	< 0.0001	< 0.0001
BLOOD DC VS. IMGL	< 0.0001	< 0.0001	< 0.0001	0.0256	< 0.0001	< 0.0001
BLOOD DC VS. FETAL MG	< 0.0001	< 0.0001	< 0.0001	0.0001	< 0.0001	< 0.0001
BLOOD DC VS. ADULT MG	< 0.0001	< 0.0001	< 0.0001	< 0.0001	< 0.0001	< 0.0001
IMGL VS. FETAL MG	< 0.0001	> 0.9999	0.9483	0.0256	0.0633	< 0.0001
IMGL VS. ADULT MG	< 0.0001	0.8258	0.3015	0.0001	0.0633	< 0.0001
FETAL MG VS. ADULT MG	0.9987	0.9431	0.1407	0.2995	> 0.9999	0.9998
COMPARISONS	**PROS1**	**APOE**	**SLCO2B1**	**SLC7A8**	**PPARD**	**CRYBB1**
CD14+ M VS. CD16+ M	0.8814	> 0.9999	0.9999	> 0.9999	0.4125	0.0011
CD14+ M VS. BLOOD DC	0.4077	0.9103	0.9994	0.9965	0.9185	0.6963
CD14+ M VS. IMGL	< 0.0001	< 0.0001	< 0.0001	< 0.0001	< 0.0001	< 0.0001
CD14+ M VS. FETAL MG	< 0.0001	< 0.0001	< 0.0001	< 0.0001	< 0.0001	< 0.0001
CD14+ M VS. ADULT MG	< 0.0001	< 0.0001	< 0.0001	< 0.0001	< 0.0001	< 0.0001
CD16+ M VS. BLOOD DC	0.9391	0.9455	0.9941	0.9987	0.138	0.0002
CD16+ M VS. IMGL	< 0.0001	< 0.0001	< 0.0001	< 0.0001	< 0.0001	< 0.0001
CD16+ M VS. FETAL MG	< 0.0001	< 0.0001	< 0.0001	< 0.0001	< 0.0001	< 0.0001
CD16+ M VS. ADULT MG	< 0.0001	< 0.0001	< 0.0001	< 0.0001	< 0.0001	< 0.0001
BLOOD DC VS. IMGL	< 0.0001	< 0.0001	< 0.0001	< 0.0001	< 0.0001	< 0.0001
BLOOD DC VS. FETAL MG	< 0.0001	< 0.0001	< 0.0001	< 0.0001	0.0004	< 0.0001
BLOOD DC VS. ADULT MG	< 0.0001	< 0.0001	< 0.0001	< 0.0001	< 0.0001	< 0.0001
IMGL VS. FETAL MG	0.0008	< 0.0001	0.2803	0.0127	0.091	> 0.9999
IMGL VS. ADULT MG	0.2533	< 0.0001	0.9909	0.4987	0.403	< 0.0001
FETAL MG VS. ADULT MG	0.1787	> 0.9999	0.7213	0.4966	0.9658	< 0.0001

Table S1. Related to Figure 2. Adjusted *p*-values for 12 genes across all groups. one-way ANOVA followed by Tukey's *post-hoc* test. * $p<0.05$, **$p<0.001$, ***$p<0.0001$.

Table S2: ELISA cytokine values (pg/ml) from conditioned media of stimulated iMGLs.

	Treatments[1]							
	Vehicle		IFNγ		IL-1β		LPS	
Cytokines	**mean ± SE**	**p-value**	**mean ± SE**	**p-value**	**mean ± SE**	**p-value**	**mean ± SE**	**p-value**
TNFα	2.56 ± 0.16	NA	58.82 ± 8.80	0.0008	29.74 ± 0.65	0.0471	116.49 ± 9.77	< 0.0001
IL6	0.00 ± 0.00	NA	12.22 ± 1.44	0.5649	13.92 ± 0.41	0.4736	274.39 ± 15.25	< 0.0001
IL8	339.21 ± 11.29	NA	3549.05 ± 181.22	< 0.0001	3,004.54 ± 47.58	< 0.0001	4,347.96 ± 75.61	< 0.0001
IL10	0.00 ± 0.00	NA	4.59 ± 2.35	0.1599	4.42 ± 1.33	0.1779	31.31 ± 1.52	< 0.0001
IL1α	1.59 ± 0.07	NA	1.48 ± 0.25	0.9999	4.89 ± 1.45	0.2535	30.55 ± 2.19	< 0.0001
CCL2	96.59 ± 6.27	NA	993.26 ± 55.76	0.0052	275.98 ± 19.54	0.7069	5,695.46 ± 275.72	< 0.0001
CCL3	104.91 ± 7.70	NA	295.39 ± 19.72	0.0043	556.24 ± 54.01	< 0.0001	0.00 ± 0.00	0.0807
CCL4	3,140.81 ± 165.84	NA	4,514.72 ± 10.01	< 0.0001	4,492.26 ± 51.35	< 0.0001	4,594.57 ± 33.96	< 0.0001
CXCL10	9.62 ± 1.48	NA	0.00 ± 0.00	0.1762	69.49 ± 4.73	< 0.0001	73.72 ± 4.53	< 0.0001
CCL17	4.70 ± 0.83	NA	25.82 ± 1.98	0.0168	21.75 ± 1.94	0.0464	92.96 ± 7.70	< 0.0001

Table S2, Related to Figure 3. Elisa cytokine values (pg/ml) from conditioned media of iMGLs stimulated by IFNγ, Il-1β, and LPS for Figure 3B. Values and statistics are reported in mean ± standard error. n=3 per group. One-Way ANOVA followed by Dunnett's *post-hoc* test. Adjusted *p*-values for multiple comparisons are reported. * p<0.05, **p<0.001, ***p<0.0001.

Table S3. QPCR results of iMGLs stimulated with fAβ or BDTO.

Treatments[1]						
fAβ		**BDTO**		**fAβ vs. BDTO**		
GENES	**Fold Change (over vehicle) mean ± SE**	**Genes**	**Fold Change (over vehicle) mean ± SE**	**Genes**	**Fold difference mean**	**p-value**
MS4A6A	6.32 ± 0.32	**CD2AP**	4.62 ± 0.45	**MS4A6A**	4.731	< 0.0001
CD33	6.02 ± 0.41	**CLU**	3.84 ± 0.67	**CD33**	5.178	< 0.0001
ABCA7	5.79 ± 0.44	**BIN1**	2.56 ± 0.66	**ABCA7**	3.333	0.0014
TYROBP	4.99 ± 0.31	**ABCA7**	2.46 ± 0.70	**TYROBP**	3.756	0.0002
TREM2	4.86 ± 0.50			**TREM2**	3.426	0.0009
ZCWPW1	3.41 ± 0.42			**ZCWPW1**	2.610	0.0323
PTK2B	2.97 ± 0.16			**PTK2B**	2.483	0.0525
APOE	2.52 ± 0.19					
BIN1	2.34 ± 0.69			**CD2AP**	-4.144	< 0.0001
CLU	2.24 ± 0. 78					

[1]Treatments: fAβ (5 μg/ml) or BDTO (5 μg/ml) 24 h.

Table S3. **Related to Figure 4**. QPCR results of iMGLs stimulated with fAβ or BDTO. Results represent genes with fold change greater than 2. Results presented as mean ± standard error. n=6 per group. Two-way ANOVA followed by Sidak's *post-hoc* test. Adjusted *p*-values for multiple comparisons. * p<0.05, **p<0.001, ***p<0.0001**.**

Table S4: Top GO pathways enriched in Adult MG compared to Fetal MG and iMGLs.

Adult MG vs Fetal MG				Adult MG vs iMGL			
Description	**GO ID**	**LogP (-)**	**Log (q-value)**	**Description**	**GO ID**	**LogP (-)**	**Log(q-value)**
Extracellular matrix organization	0030198	38.10	-34.18	Regulation of cell migration	0030334	13.23	-9.58
Circulatory system development	0072359	36.87	-33.23	Regulation of cell adhesion	0030155	11.46	-8.12
Single organism cell adhesion	0098602	32.24	-29.04	Actin filament-based process	0030029	11.03	-7.78
Regulation of nervous system development	0051960	28.56	-25.55	Regulation of anatomical structure morphogenesis	0022603	10.95	-7.74
Regulation of cellular component movement	0051270	26.49	-23.54	Cell junction organization	0034330	10.29	-7.12
Adaptive immune response	0002250	25.87	-22.96	Enzyme linked receptor protein signaling pathway	0007167	9.73	-6.76
Response to cytokine	0034097	20.02	-17.49	Circulatory system development	0072359	8.59	-5.79
Epithelial cell proliferation	0050673	19.25	-16.74	Single-organism catabolic process	0044712	8.13	-5.42
Central nervous system development	0007417	19.12	-16.63	Oxidation-reduction process	0055114	7.78	-5.11
Negative regulation of cell proliferation	0008285	18.82	-16.34	Plasma membrane organization	0007009	7.35	-4.76
Tissue morphogenesis	0048729	18.50	-16.06	Cellular response to oxygen-containing compound	1901701	7.31	-4.73
Muscle structure development	0061061	17.98	-15.56	Negative regulation of cell proliferation	0008285	7.28	-4.72
Single organism cell adhesion	0050808	17.86	-15.48	Positive regulation of phosphorylation	0042327	7.14	-4.63
Regulation of nervous system development	0042063	17.26	-14.91	Renal system development	0072001	6.77	4.30
Regulation of Growth	0040008	16.62	-14.32				

Table S4. Related to Figure 2. Gene ontology terms enriched in Adult MG vs Fetal MG and iMGL.

Table S5: Top GO pathways enriched in Fetal MG compared to Adult MG and iMGL.

Fetal vs Adult MG				Fetal MG vs iMGL			
Description	**GO ID**	**LogP (-)**	**Log (q-value)**	**Description**	**GO ID**	**LogP (-)**	**Log(q-value)**
Leukocyte chemotaxis	0030595	6.92	-3.07	Single-organism catabolic process	0044712	10.41	-6.64
Response to acidic pH	0010447	4.07	-1.33	Regulation of cell migration	0030334	9.90	-6.26
Inorganic ion homeostasis	0098771	4.04	-1.31	Iron ion transport	0006826	8.68	-5.52
Regulation of cell migration	0030334	3.80	-1.18	Divalent metal ion transport	0070838	8.44	-5.34
Circulatory system process	0003013	3.72	-1.13	Carbohydrate metabolic process	0005975	7.39	-4.59
Melanosome organization	0032438	3.70	-1.13	Small GTPase mediated signal transduction	0007264	6.69	-3.99
Anion transport	0006820	3.54	-1.01	Angiogenesis	0001525	6.64	-3.97
Macrophage migration	1905517	3.47	-0.95	Positive regulation of transport	0051050	6.15	-3.59
Transmembrane receptor protein tyrosine kinase signaling pathway	0007169	3.23	-0.81	Positive regulation of intracellular signal transduction	1902533	6.12	-3.57
Negative regulation of receptor activity	2000272	3.14	-0.76	Aminoglycan metabolic process	0006022	6.03	-3.50
Positive regulation of phagocytosis, engulfment	0060100	3.13	-0.76	Cell projection assembly	0030031	5.81	-3.31
Sterol import	0035376	3.13	-0.76	Cell-substrate adhesion	0031589	5.68	-3.21
Behavior	0007610	3.11	-0.75				
Positive regulation of transport	0051050	3.02	-0.70				
Vesicle organization	0016050	2.96	-0.65				

Table S5. Related to Figure 2. Gene ontology terms enriched in Fetal MG vs Adult MG and iMGL.

Table S6: Top GO pathways enriched in iMGL compared to Fetal MG and Adult MG.

iMGL vs Fetal MG				iMGL vs Adult MG			
Description	**GO ID**	**LogP (-)**	**Log (q-value)**	**Description**	**GO ID**	**LogP (-)**	**Log(q-value)**
Single organism cell adhesion	0098602	30.48	-26.23	Mitotic cell cycle process	1903047	28.46	-24.22
Mitotic cell cycle process	1903047	21.34	-17.87	Regulation of cell cycle	0051726	19.26	-15.94
Immune system development	0002520	18.56	-15.55	DNA replication	0006260	17.22	-14.09
Regulation of cellular component movement	0051270	16.11	-13.32	Chromatin organization	0006325	11.44	-8.64
Mitotic cell cycle phase transition	0044772	15.94	-13.18	Regulation of nuclear division	0051783	11.25	-8.47
Leukocyte migration	0050900	15.19	-12.49	Immune system development	0002520	10.90	-8.15
Taxis	0042330	14.76	-12.12	DNA-dependent DNA replication	0006261	10.22	-7.51
Positive regulation of cell differentiation	0045597	14.76	-12.12	Negative regulation of transcription from RNA polymerase II promoter	0000122	10.20	-7.50
Inflammatory response	0006954	14.64	-12.03	Microtubule cytoskeleton organization	0000226	9.96	-7.27
Anatomical structure formation involved in morphogenesis	0048646	13.83	-11.27	Leukocyte activation	0045321	9.57	-6.94
Positive regulation of cell proliferation	0008284	13.82	-11.26	Regulation of small GTPase mediated signal transduction	0051056	9.16	-6.56
Positive regulation of intracellular signal transduction	1902533	12.20	-9.73	Cell cycle G2/M phase transition	0044839	9.01	-6.44
Positive regulation of hydrolase activity	0051345	11.80	-9.35	Signal transduction by p53 class mediator	0072331	8.47	-5.99
Negative regulation of multicellular organismal process	0051241	11.67	-9.23	Regulation of transcription involved in G1/S transition of mitotic cell cycle	0000083	8.34	-5.88
Negative regulation of cell proliferation	0008285	11.62	-9.18	Cellular response to oxygen-containing compound	1901701	8.15	-5.73

Table S6. Related to Figure 2. Gene ontology terms enriched in iMGL vs Fetal MG and Adult MG.

Table S7: QPCR Primers for AD-GWAS gene expression changes attributed to fAβ or BDTO.

Gene	Identifier	Source
APOE	Hs00171168_m1	Taqman
ABCA7	Hs01105117_m1	Taqman
BIN1	Hs00184913_m1	Taqman
CASS4	Hs00220503_m1	Taqman
CD2AP	Hs00961451_m1	Taqman
CD33	Hs01076281_m1	Taqman
CLU	Hs00156548_m1	Taqman
CR1	Hs00559342_m1	Taqman
DSG2	Hs00170071_m1	Taqman
INPP5D	Hs00183290_m1	Taqman
PICALM	Hs00200318_m1	Taqman
PTK2B	Hs00169444_m1	Taqman
MEF2C	Hs00231149_m1	Taqman
MS4A6A	Hs01556747_m1	Taqman
MS4A4A	Hs01106863_m1	Taqman
TREM2	Hs00219132_m1	Taqman
TREML2	Hs01077557_m1	Taqman
TYROBP (DAP12)	Hs00182426_m1	Taqman
ZCWPW1	Hs00215881_m1	Taqman

Table S7. Related to STAR Methods. QPCR Primers AD-GWAS gene expression analysis.

Movie S1. Related to Figure 7. Z-slice of iMGLs interacting with Aβ plaques in AD transgenic mice. Confocal Z-series demonstrates the intimate interactions that occur between transplanted iMGLs (red) and fibrillar Aβ plaques (white) in Rag-5xfAD mice.